Available online at www.sciencedirect.com
ScienceDirect
Ceramics International 37 (2011) 3535–3545
CERAMICS INTERNATIONAL
www.elsevier.com/locate/ceramint

Electromagnetic absorption, reflection and interference shielding in X-band frequency range of low cost ceramic building bricks and sandwich type ceramic tiles using mill scale waste as an admixture

G. Bantsis [a], C. Sikalidis [a,*], M. Betsiou [a], T. Yioultsis [b], Th. Xenos [b]

[a] Department of Chemical Engineering, Aristotle University of Thessaloniki, 54006, Thessaloniki, Greece
[b] Department of Electrical & Computer Engineering, Aristotle University of Thessaloniki, 54006, Thessaloniki, Greece

Received 10 May 2011; accepted 6 June 2011
Available online 12 June 2011

Abstract

General concern for potential health effects of 24 h electromagnetic fields (EMF) exposure has increased over the recent years. This has led to the necessity of developing low cost electromagnetic interference (EMI) shielding and especially absorbing building materials. In the present study the utilization of steel mill scale waste in ceramic bricks for this purpose was investigated, while the development of an improved, regarding mainly absorption performance, building material also occurred. Both ceramic bricks and sandwich type ceramic tiles were found to have good shielding efficiency and absorption performances in the same X-band frequency range (8–12 GHz) while technological and environmental requirements as building materials were also established.

Keywords: C. Electrical properties; C. Mechanical properties; D. Ferrites; D. Traditional ceramics

1. Introduction

Over the past decades, research on electromagnetic fields (EMF) has been motivated primarily by public health considerations. There is a general public concern about potential health effects of daily exposure, especially for sensitive groups in human population such as children and adults. For adults especially due to their occupational exposure to EMF from mobile phone base stations, radio and television transmitters and occupational transmitters such as, PVC welding machines, plasma etching and military and civil radar systems, all operating at different frequencies even if the exposure levels are orders of magnitude lower than the exposure from the device (e.g. phone) itself [1].

In recent years, work has been focused on possible effects at nonthermal levels or under conditions in which physiologic temperature can be maintained in the presence of normally thermalizing specific absorption rates (SAR). Studies of human perception indicate that the greatest cutaneous sensitivity to microwave (MW) heating is at frequencies with wavelengths comparable to or smaller than the thickness of skin, the millimeter wave range [1]. At frequencies, 1–10 GHz, with wavelengths equal to or longer than the human body, much of the energy is absorbed below the superficial dermis. In this range, the threshold temperature for cellular injury (about 42 °C) is below the threshold for pain (about 45 °C). Consequently cutaneous perception of RF energy may not be a reliable response, which protects against potentially harmful levels of RF radiation at the lower microwave frequencies [2,3].

Furthermore, EMI shielding is in critical demand due to the interference of wireless (particularly radio frequency) devices with digital devices and the increasing sensitivity and importance of electronic devices [4]. Numerous studies have been carried out over the recent years into the development of cement based electromagnetic shielding and absorbing materials containing wastes in general as an admixture [5], Nevertheless, few studies have been reported regarding construction absorbing materials and especially in the field of ceramics (bricks, tiles, etc.) [6–11].

Finally, the objective of this study was (i) to characterize the mill scale produced by a Greek steel plant, (ii) to develop low cost ceramic building bricks using steel mill scale as an admixture, (iii) to investigate their use as a shielding and especially

* Corresponding author. Tel.: +30 2310996185; fax: +30 2310996230.
E-mail addresses: sikalidi@auth.gr, sikalidi@eng.auth.gr (C. Sikalidis).

0272-8842/$36.00
doi:10.1016/j.ceramint.2011.06.010

absorbing material in X-band frequency range (8–12 GHz) using free space measurements, (iv) to develop a new low cost ceramic building sandwich type tile using the same waste as an admixture that increases its shielding and especially absorption performance, in the same frequency range, (v) to maintain, as much as possible, the technological characteristics of this new products according to international standards and procedures and (iv) to examine if these new products are environmentally accepted.

2. Materials and methods

2.1. Waste sampling and analysis

In order to investigate the chemical and mineralogical characteristics of steel mill scale (ms) waste, average samples were taken every month from the baghouse of a Greek steel plant [12]. The samples were mixed and homogenized in a cone mixture and dried in an industrial dryer at 110 °C peak temperature. The ms waste samples were kept in plastic sealed drums in order to be used for the preparation of the ceramic specimens (bricks).

The chemical compositions were determined by using a Perkin Elmer AAnalyst 800 atomic absorption spectrophotometer either with flame or graphite furnace. Mineralogical analysis of samples and specimens were performed by using a Philips PW 1820/00 diffractometer equipped with a PW1710/00 controller. CuKα radiation and a Ni-filter were used. The samples were scanned over an interval of 3–63° 2θ at a scanning speed of 1.2°/min. The behaviour of ms and clayey material at elevated temperatures was investigated through thermogravimetric (TG) analysis using a Perkin Elmer STA 6000 Thermal Analyzer. Nitrogen (99.999% N_2) was used as the inert gas, and 10% O_2 in N_2 was used as the oxidizing gas. SEM-EDX study was performed by using a Scanning Electron Microscope (JEOL JSM-840) connected to an X-ray Energy Dispersion Spectrometer-EDS (LINK-AN 10000). Finally, particle size analyses were performed, using an Endecott's vibrating shaker and the relevant testing sieves.

2.2. Ceramic bricks for technological properties

For the determination of the technological characteristics of the products, two sets of ceramic bricks (10 × 10 × 3 cm) were prepared as follows. 360 g of clayey powder and 0, 5, 10, 15, 20 wt% additions of ms waste with random particle size were thoroughly mixed and homogenized. Water was added to prepare a ceramic mass with a moisture content of 7 wt%, which was shaped by press-forming at 400 kg/cm^2, using a 10 × 10 × 8 cm stainless steel mold and a 45 tn carver laboratory press. The bricks were dried in a box dryer at 110 °C for 24 h. Shaped ceramic bricks were subjected to thermal treatment, at the peak temperatures of 800, 850, 900, 950, 1000 and 1050 °C for 4 h in a Thermconcept kc 32/13 box kiln. Fired ceramic bricks were tested for water absorption, firing shrinkage compressive strength and modulus of rupture according to European standard methods and procedures [13–16]. The firing schedule that gave the best properties was chosen for the experiments that followed.

Finally, a second set of ceramic bricks was prepared with the same additions and 0.1, 0.25, 0.5, 1.0, 1.4 and 2.0 mm particle size of ms waste using the prementioned procedure in order to determine the best percentage addition and particle size of ms for achieving optimum technological properties.

2.3. Ceramic bricks and tiles for EMI measurements

Having determined the best percentage addition (15 and 20 wt%) and particle size of ms waste (0.5 mm), ceramic bricks for EMI measurements were prepared according to the prementioned procedure. The pressing load of 400 kg/cm^2 and firing schedule of 4 h at 1000 °C were selected because under this process higher percentage of magnesioferrite was developed within ceramic bricks. Using 18 ceramic bricks, two small walls with different ms waste additions were constructed by using plain Portland cement type A as the conjunctional material (Fig. 1a). Afterwards, by raising the pressing load to 500 kg/cm^2 and following the same procedure, thicker ceramic tiles were prepared. Each ceramic tile was pieced together with one ceramic tile of same ms waste addition with the use of Portland cement type A (1 cm in thickness), which was initially mixed and homogenized in a cone mixture with 10 wt% ms waste (0.1 mm particle size), as the conjunctional material. From this procedure, the ceramic sandwich type tiles that were constructed had almost the same total amount in ms waste with the similar ceramic bricks while all other characteristics remained almost stable (Table 1). Using 18 of the pre-mentioned ceramic sandwich type tiles, two small double tile walls containing different percentages of ms waste were constructed by using plain Portland cement type A as the conjunctional material (Fig. 1b). Finally the remaining ceramic sandwich type tiles were used for the investigation of their technological characteristics as presented below.

Table 1
Characteristics of ceramic bricks and sandwich tiles.

	ms waste (wt%)	Dimensions (cm)	Total weight (g)	Weight in ms waste (g)	Volume (cm^3)	Density (g/cm^3)
Bricks	15	10 × 10 × 3	360	54	300	1.2
	20	10 × 10 × 3	360	72	300	1.2
Cement paste	10	10 × 10 × 1	100	10	100	1
Sandwich tiles	15	10 × 10 × 3	460[a]	64[a]	300	1.53[a]
	20	10 × 10 × 3	460[a]	82[a]	300	1.53[a]

[a] Small increment due to cement paste.

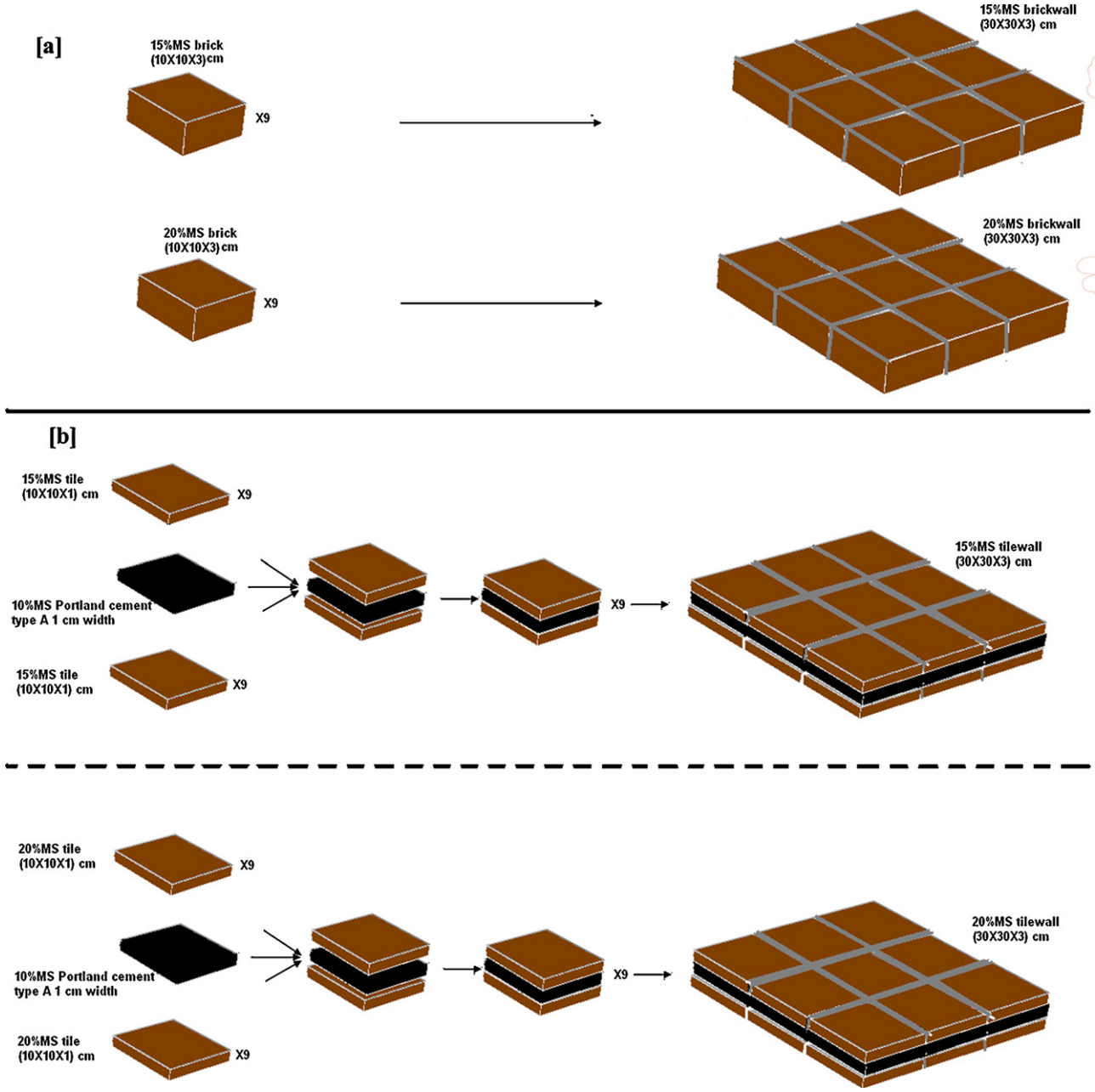

Fig. 1. Schematic presentation of the construction of (a) small ceramic brick walls and (b) tile walls from small dimensioned ceramic bricks and tiles with different percentage in addition of ms waste and 0.5 mm particle size.

2.4. Shielding efficiency (SE), absorption and reflection measurements

For a better approximation of real conditions (e.g. houses near radio and television transmitters) a free-space measurement approach was chosen. From the measurement of S-parameters, shielding efficiency and absorption–reflection coefficients of the ceramic brick–tile walls were calculated. The 4 small dimensioned brick and tile walls were clamped on a home-made sample holder (brass) and were placed at a distance of 10 cm from the edge of the radiating antenna and equally 10 cm from the edge of the receiving antenna to approximately ensure free space conditions. The sample position is at the maximum of the beam where the field can be considered planar and the incidence normal (Fig. 2). Using the vector network analyzer, the S-parameters, S_{11} and S_{21}, were measured. Reflection coefficient, R, and transmission coefficient, T, are given as $R = |S_{11}|^2$ and $T = |S_{21}|^2$. The absorption coefficient, A, can be obtained from the simple relation $A + R + T = 1$. The EMI shielding efficiency, SE, is defined as the ratio of the power of the incident wave P_I to that of the transmitted wave P_T [17].

$$\mathrm{SE} = 10 \log \left(\frac{P_I}{P_T} \right) \mathrm{dB} \quad (1)$$

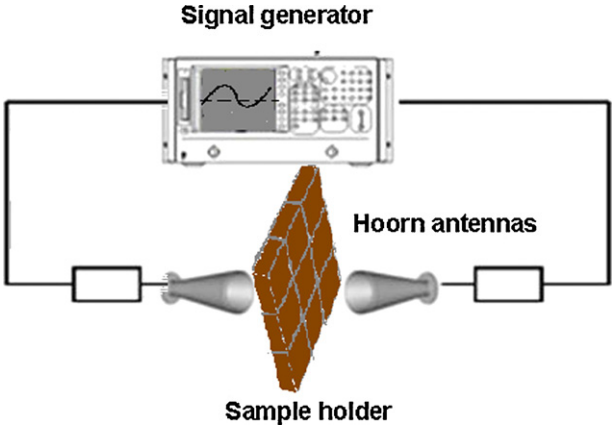

Fig. 2. Schematic presentation of the SE, absorption and reflection measurements for the 8–12 GHz frequency range.

2.5. Technological characteristics (water absorption, flexural and compressive strength, firing shrinkage) of ceramic building sandwich type tiles

All tests were performed according to European standardized methods and procedures [13–16] while the obtained results were compared to the relevant specifications.

2.6. Leaching test

Leaching tests on ms waste, ceramic bricks and sandwich type tiles containing 20 wt% ms waste of 0.5 mm particle size, were performed according to EN 12457 [18].

3. Results and discussion

3.1. Chemical, mineralogical and thermogravimetric analysis

The results of chemical analysis of ms waste samples and clayey material are given in Tables 2 and 3, respectively. Iron found to dominate in ms, which is common in these types of wastes [19]. The sum of iron oxides in all samples exceeds 96 wt%. Chemical, mineralogical, particle size and thermogravimetric analysis showed that clayey material is typical for such applications (Tables 3–5 and Figs. 3 and 4) [20]. Main phases identified within ms (Fig. 3) found to be FeO and Fe_3O_4. TG analysis of ms presented a small weight increase of 2% due to partial oxidation of magnetite–wursite mixture to hematite (above 550 °C), although the oxidation of pure magnetite leads to a weight gain of 3.455% [21]. Furthermore, the low-temperature oxidation of magnetite particles did not occur, due to the impure magnetite and its large particle size (Fig. 4, insert).

3.2. Effect of firing temperature on the technological characteristics of ceramic bricks

The temperature of 1050 °C was found to be critical for this ceramic mass, because above this temperature the ceramic body started to become over-fired. Water absorption of ceramic bricks containing ms varied between 8 and 11% and considered to be within accepted limits. The increase of ms addition resulted to a decrease of water absorption (at temperatures above 900 °C), suggesting a fluxing action of ms waste. Additions from 5 to 20 wt% resulted to a water absorption decrease from 11 to 8 wt% as firing temperature was raised, while bricks without any addition presented water absorption between 12 and 10 wt% (Fig. 5a). Firing shrinkage values were also improved as firing temperature and the addition of ms increased respectively and varied between 0.5 and 2.0% (Fig. 5b). This small firing shrinkage values were attributed mainly to ceramic mass. Mill scale wastes were formed from industrial procedures of higher temperatures in comparison to the firing temperature of ceramic bricks (1050 °C maximum fired temperature). Consequently, the presence of ms wastes is not expected to affect considerably the firing shrinkage of the ceramic bricks. Flexural and compressive strength values were also found to improve with the increment of ms additions up to 20 wt% (Fig. 5c, d). Modulus of rupture and compressive strength values showed an intense increase at temperatures above 900 °C, also indicating the starting of the fluxing action of ms at this temperature. In the same temperature range 900–

Table 2
Chemical composition of ms waste samples (wt%).

Sample no.	FeO	MnO	Cr_2O_3	CaO	Al_2O_3	SiO_2	Na_2O	K_2O	P_2O_5	MgO
1	97.35	0.89	0.09	0.16	0.44	0.87	0.04	0.07	0.05	0.04
2	97.32	0.63	0.11	0.29	0.28	0.96	0.09	0.08	0.17	0.07
3	96.83	0.82	0.14	0.35	0.49	1.19	0.02	0.08	0.03	0.05
4	97.17	0.66	0.08	0.25	0.62	0.96	0.06	0.09	0.08	0.03

Table 3
Chemical composition of clayey material (wt%).

Fe_2O_3	CaO	Al_2O_3	SiO_2	Na_2O	K_2O	MgO	LOI[a]
1.48	7.32	12.45	58.68	0.50	3.80	7.20	8.57

[a] Loss on ignition.

Table 4
Particle size analysis of clayey material and ms.

Particle size (mm)	Clayey material (wt%)	Mill scale (wt%)
>2.0	0.37	18.23
2.0–1.4	0.91	23.61
1.4–1.0	1.89	19.25
1.0–0.5	3.48	17.29
0.5–0.25	22.0	15.32
0.25–0.1	30.50	4.0
<0.1	40.85	2.3

Table 5
Some magnetic properties of iron-based oxides.

Oxides	Composition	Magnetic order	T_c (°C)	s_s (A m^2/kg)
Magnetite	Fe_3O_4	Ferrimagnetic	575–585	90–92
Hematite	Fe_2O_3	Canted AFM	675	0.4
Magnesioferrite	$MgFe_2O_4$	Ferrimagnetic	440	21

AFM = antiferromagnetic order. T_c = Curie or Neel temperature. s_s = saturation magnetization at room-temperature.

950 °C, magnesioferrite was formed. Mineralogical analysis of the bricks containing 20 wt% ms and fired at 800, 900 and 1000 °C respectively, indicated the beginning of the formation of magnesioferrite at 900 °C. This was amplified at 1000 °C (Fig. 6). When peak firing temperature raised, peaks in the XRD pattern became sharper and more intense, although the formation of magnesioferrite considered to be partial, due to lack of equimolar amounts of MgO and Fe_2O_3 and appropriate oxygen pressure conditions in general [22]. The SEM-EDX

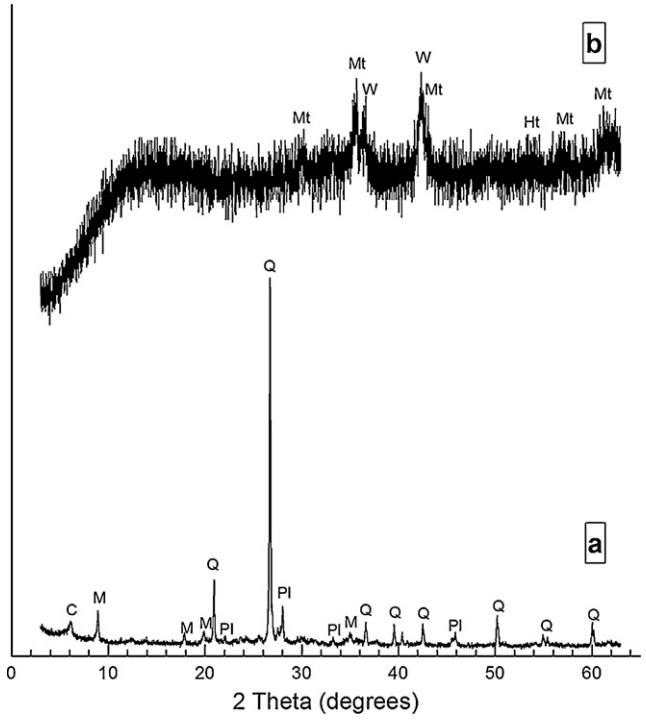

Fig. 3. X-ray diffractogram of: (a) clayey material (main phases identified: Tc, total clays; Q, Quartz; M, mica and Pl, Plagioclase), (b) ms waste dust samples (main phases identified: Mt, magnetite and W, wursite).

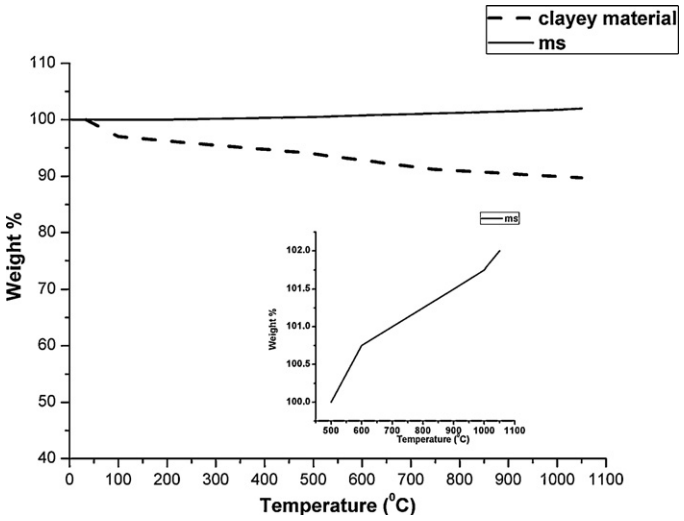

Fig. 4. Thermogravimetric analysis of clayey material and ms waste fired at 1050 °C. Insert – thermogravimetric analysis of ms waste fired from 500 to 1050 °C.

(Fig. 7) showed areas of ceramic brick fired at 950 °C, with increased concentration of Mg and Fe (a), as well as areas where Fe dominates (b). The above supports the possible presence of magnesioferrite and hematite respectively, in these areas. The formation of magnesioferrite is connected to the increase of the ceramic structure strength which is supported from the increment of modulus of rupture and compressive strength values of bricks fired above 900 °C.

Furthermore, flexural strength of the fired bricks without any ms waste addition increased as the firing temperature raised respectively (up to 1050 °C). The colour of the ceramic bricks was turned from red to medium brown with the increase in ms addition and the increase of firing temperature. These colours are accepted in the market of clay bricks (Fig. 8). Finally, taking in consideration the production cost and the results of the technological tests presented, the peak firing temperature of 1000 °C was chosen as the optimum.

3.3. Effect of percentage addition and particle size of ms on the technological properties of ceramic bricks fired at 1000 °C

The results of the technological tests are presented in Fig. 9. Water absorption of the ceramic bricks was affected from the different ms waste additions and particle sizes (Fig. 9a). Especially particle size appeared to be the primary factor. For particle sizes 0.1–1.4 mm (5–20 wt% ms waste additions), water absorption was decreased from 10.5 to 7.5%, values which are considered to be within acceptable limits. Best results were obtained for 0.5 mm particle size and 20 wt% ms waste suggesting a positive action of ms waste. Furthermore, regarding ceramic bricks that contained ms waste with particle size > 2 mm, 15% water absorption was reached, which considered to be apart from accepted limits. This was attributed mainly to the iron oxides in ms waste and to large particle size (2.0 mm). During press forming due to iron oxides presence,

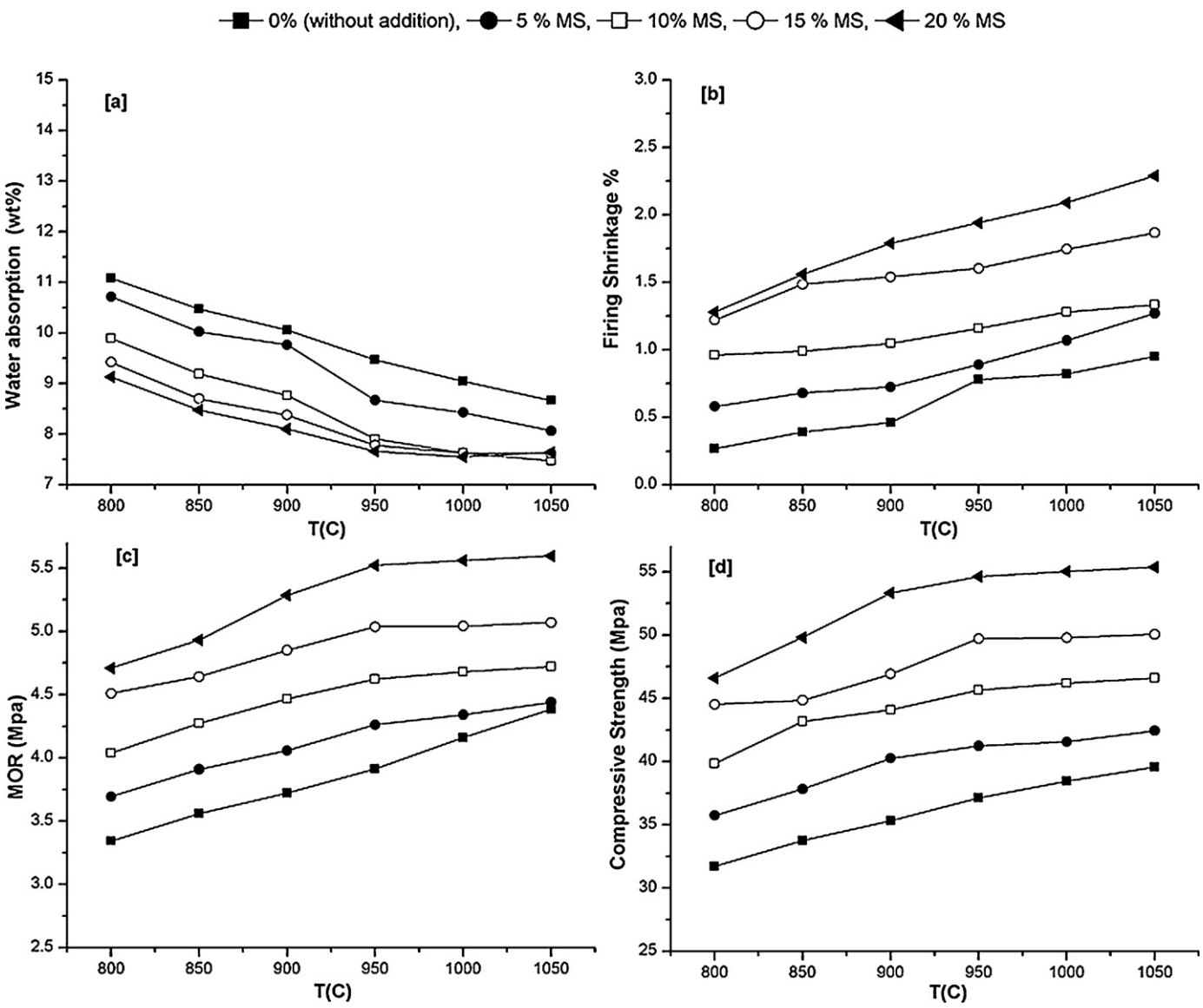

Fig. 5. Effect of firing temperature on the: (a) water absorption, (b) firing shrinkage, (c) modulus of rupture values (MOR) and (d) compressive strength of ceramic bricks containing different percentages of ms.

small voids were formed. The presence of these voids after sintering increased the porosity and consequently water absorption of the bricks while flexural and compressive strength were also decreased (Fig. 9c, d). On the contrary bricks containing 5 wt% ms waste with particle size of 2.0 mm, presented values in the same order of magnitude with bricks containing ms with smaller particle size. This was attributed mainly to the small percentage of ms waste and the highly sintered ceramic mass that was achieved with the firing schedule used (1000 °C, 4 h). Finally, firing shrinkage values varied from 1.3 to 2.0% and raised with the increment of percentage addition in ms waste (Fig. 9b). These low values suggested small tolerances in the size of the final product.

3.4. Shielding efficiency (SE)

The variation in EMI shielding of two brick walls and two tile walls with different wt% ms waste in the same X-band frequency range were measured (Fig. 10a, b). The higher the SE value in decibels, the lower the energy passing through the sample. All measured SEs can be considered as the combination of the electromagnetic (EM) radiation, i.e. reflection from the material's surface, absorption of the EM energy and multiple internal reflections of the EM radiation [17]. It was evident from Fig. 10a, b that SE was improved with the increment of ms waste addition. SE for these ceramic materials was attributed mainly to the existence of hematite and magnesioferrite (Fe_2O_3, $MgFe_2O_4$) that were formed based in previous studies [4,5]. Average SE for brick walls (3 cm thick) found to be 3 dB for 15 wt% ms waste while for brick wall containing 20 wt% ms waste 4 dB average SE was achieved. Furthermore, by constructing a sandwich with two ceramic tiles binded with cement containing 10 wt% ms waste, SE was increased. Sandwich tile wall with tiles containing 15 wt% ms waste presented 4.5 dB average SE while with 20 wt% ms waste 8 dB average SE was achieved (Fig. 10b). This

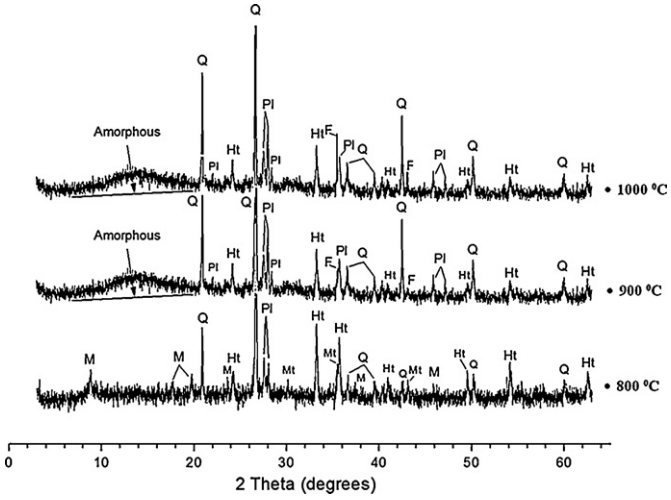

Fig. 6. X-ray diffractogram of ceramic bricks containing 20 wt% ms and fired at 800, 900 and 1000 °C for 4 h respectively. Main phases identified: Q, Quartz; Pl, Plagioclase; Ht, hematite and Mt, magnetite (800 °C), Q: Quartz, Pl: Plagioclase, Ht: hematite and F: magnesioferrite (900 and 1000 °C).

improvement in EMI shielding was attributed mainly to the conversion of one material's surface into 3 surfaces (sandwich type tiles) since the thickness and overall content of ms waste in both brick wall and sandwich type tile wall was almost the same (Table 1).

3.5. Absorption coefficient

The variation in absorption coefficient of the same dimensioned brick–tile walls were presented respectively in Fig. 10c, d. Absorption coefficient for the small dimensioned brick walls increased with the ms waste addition (15–20 wt% respectively) but the trend remained the same. The increment of electromagnetic absorption was attributed mainly to the higher percentage of magnesioferrite that was formed. Wave absorbing materials in general can be divided into three types as electric loss, magnetic loss and dielectric loss materials [23–25]. Ferrites and fine powders are magnetic loss absorbents, which attenuate and absorb electromagnetic energy by

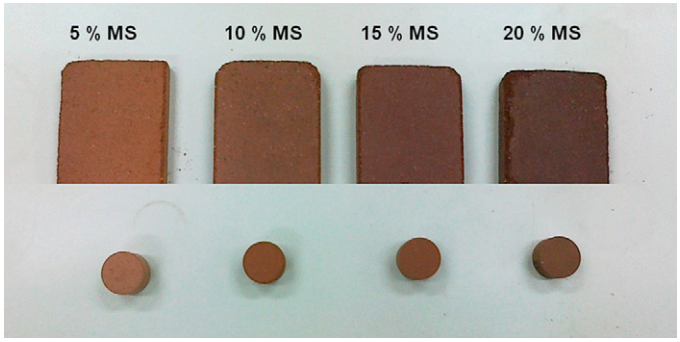

Fig. 8. Colour of ceramic bricks containing 5–20 wt% ms and fired at 1000 °C for 4 h respectively.

polarization mechanisms such as hysteresis loss and magnetic domain resonance. As presented in Table 6, magnesioferrite is ferrimagnetic and presents 0.21 A m^2/kg saturation magnetization at room-temperature [26,27]. Average electromagnetic absorption for brick wall containing 15 wt% ms waste reached 35% while for the brick wall containing 20 wt% ms waste, 50% average electromagnetic reduction due to absorption, was achieved. Proportionally, as presented in Fig. 10d, by simply dividing the small ceramic brick into 2 ceramic tiles and using plain cement with 10 wt% ms waste as the conjunctional material average electromagnetic absorption was increased. Specifically, for ceramic tile wall containing 15 wt% ms waste 50% average absorption was reached, while for double tile wall containing 20 wt% ms waste, 80% average absorption was achieved. The increment in absorption performance was attributed to the presence of magnetite containing in cement paste due to ms waste (Fig. 3), material which is highly ferrimagnetic (Table 5), as well as to the formation of magnesioferrite which also occurred. Furthermore, although maximum electromagnetic absorption was increased, stabilization in absorbing electromagnetic radiation was reduced (from 8.75 GHz for brick walls to 10.5 GHz for double tile walls). This phenomenon was attributed to the small size of the ceramic tiles (1 cm in thickness) which led to the increment of multiple internal reflections of the EM radiation.

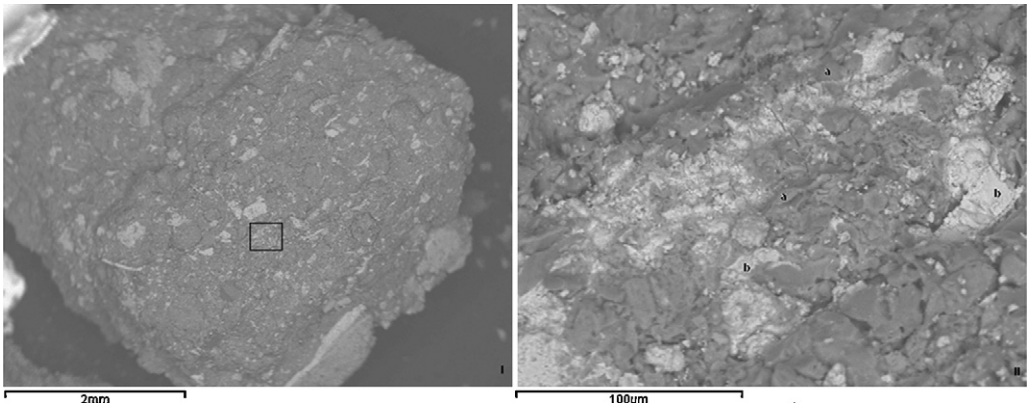

Fig. 7. Scanning Electron Image (backscattered) of areas of ceramic brick (I–II) containing 20 wt% ms and fired at 950 °C for 4 h. Areas (a) present increased concentration of Mg and Fe and (b) present increased concentration of Fe.

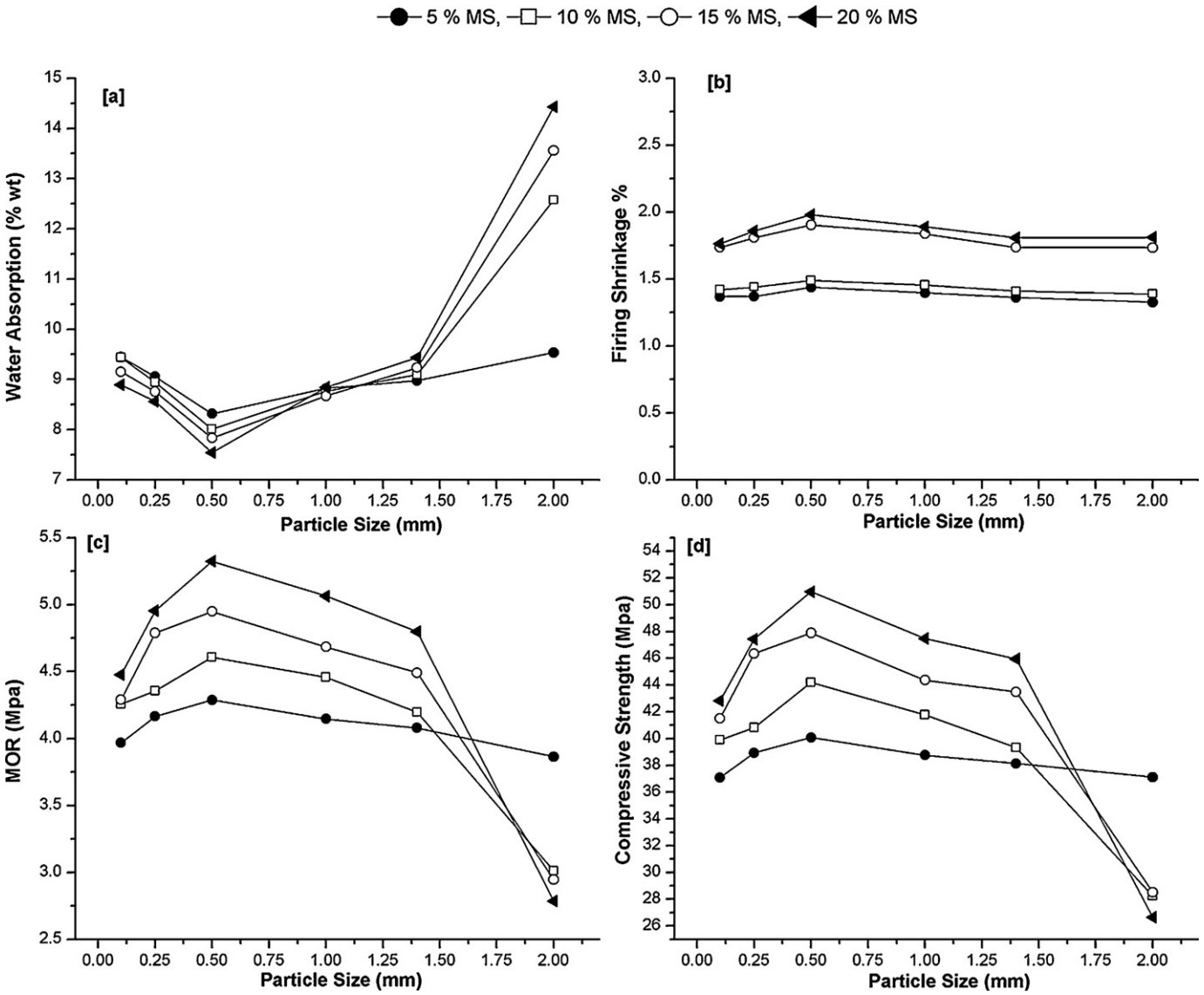

Fig. 9. Effect of percentage addition and particle size of ms on the: (a) water absorption, (b) firing shrinkage, (c) modulus of rupture values (MOR) and (d) compressive strength of ceramic bricks fired at 1000 °C.

3.6. Reflection coefficient

Reflection measurements were presented to be frequency depended. Furthermore, it was evident from Fig. 10e that reflection coefficient was not affected from the increment in ms waste addition. On the other hand, the use of cement as the conjunctional material in the construction of ceramic sandwich type tiles increased the whole conductivity of the double ceramic tile walls, therefore the impedance matching between the material surface and the free space was improved. Finally, a small increment in reflection performance regarding ceramic sandwich type walls was attributed mainly to the presence of iron particles containing in cement paste due to ms waste (Fig. 10f).

Table 6
Water absorption (WA), modulus of rupture values (MOR), compressive strength values (Cs) and firing shrinkage values (Fs) of ceramic sandwich type tiles containing 15–20 wt% in addition and 0.5 mm particle size of ms waste respectively.

Ceramic sandwich type tiles	15 wt% ms		20 wt% ms	
	Mean	Standard deviation	Mean	Standard deviation
WA (wt%)	9.811	0.052	9.313	0.103
MOR (Mpa)	4.491	0.047	4.865	0.063
Cs (Mpa)	43.093	0.320	47.486	0.474
Fs (%)	1.432	0.038	1.482	0.007

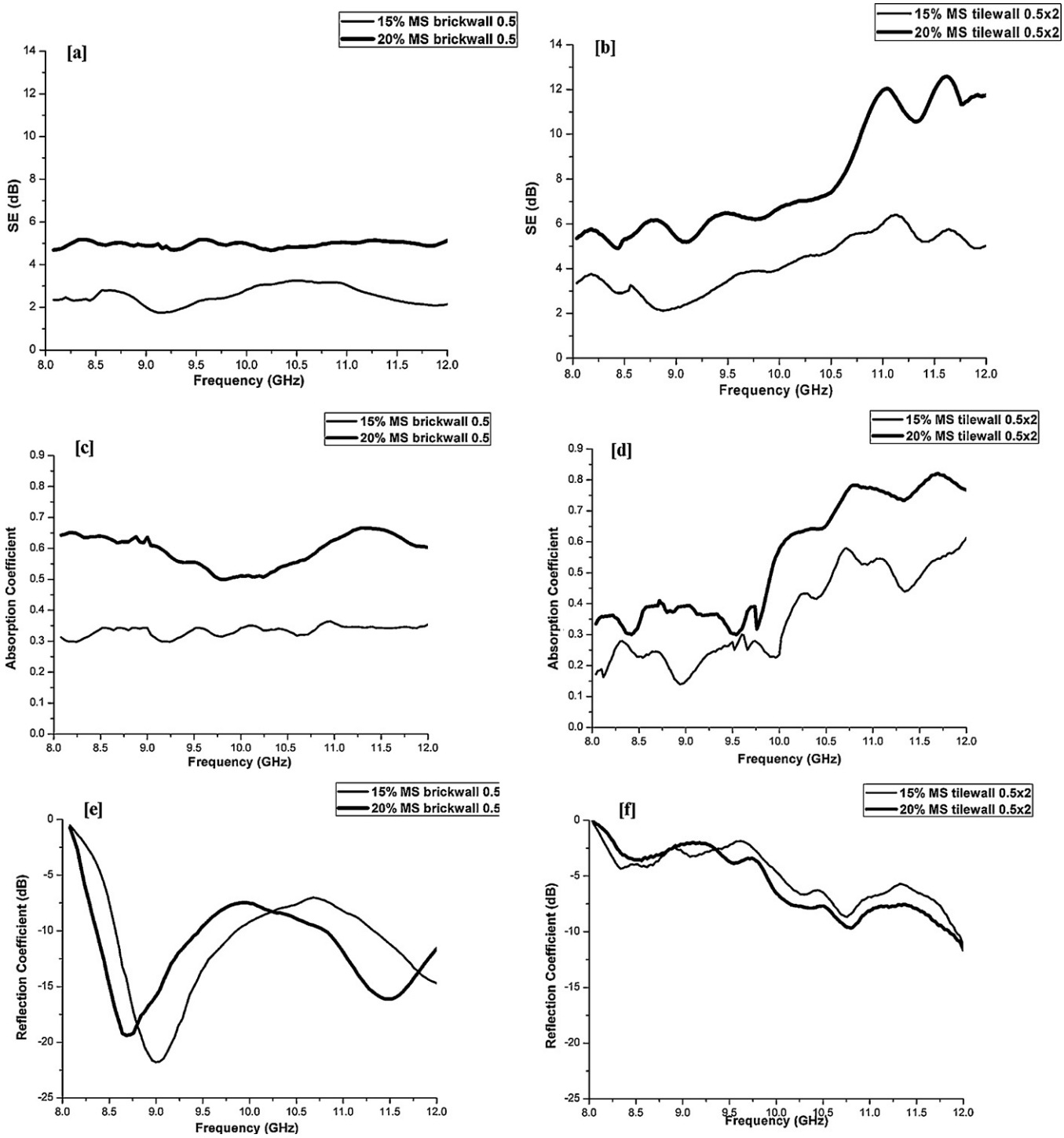

Fig. 10. (a–f) SE, variation of absorption and reflection coefficient of brick walls and sandwich type tile walls.

3.7. Technological characteristics (water absorption, flexural and compressive strength, firing shrinkage) of ceramic sandwich type tiles

Water absorption values in sandwich type ceramic tiles varied between 9 and 10% and considered to be within accepted limits while for similar ceramic bricks found between 7.5 and 8%. This small increment was attributed mainly to cement paste that was used as the conjunctional material. In general, flexural and compressive strength values, although were considered to be within accepted limits, were reduced about 10% in comparison with the relevant values of the ceramic bricks. This phenomenon was attributed mainly to the presence of iron oxides containing in cement paste due to ms waste. During mixing procedure with the portland cement, due to the strong nature of the iron oxides (Fe_3O_4: 5.5–6.5 Mohs scale in pure form), small gaps were formed. These small gaps led to the reduction in compressive and flexural strength values of the

Table 7
Leaching test results of ms, ceramic bricks and sandwich type tiles.

Element	Quantity leached of ms waste (mg/kg)	Quantity leached of ceramic bricks (mg/kg)	Quantity leached of ceramic sandwich type tiles (mg/kg)	Increment (mg/kg)	Accepted limit (mg/kg)	Measured limit (mg/kg)
As	0.379	0.066	0.072	0.006	2	0.05
Pb	2.115	0.489	1.248	0.759	10	0.05
Mn	ND	ND	3.6	3.6	–	0.2
Cu	0.781	ND	ND	–	50	0.5
Cd	ND	ND	ND	–	1	0.03
Ni	ND	ND	ND	–	10	0.06
Cr	ND	2.284	2.284	–	10	0.06
Fe	ND	ND	ND	–	–	0.5
Zn	0.333	0.214	0.469	0.255	50	0.1

double ceramic sandwich tile. On the contrary, the partial formation of magnesioferrite increased the ceramic structure of the double ceramic sandwich type tiles as was also indicated from the increment of modulus of rupture and compressive strength values while ms waste addition was raised (Table 6). Finally, firing shrinkage values were raised with the increment of ms waste addition and varied from 1.3 to 1.5%. These values were found to be in the same order of magnitude in comparison with the values from the ceramic bricks that were presented above. Although these values are extremely low, should always be taken in consideration, due to the severity of this property regarding the design of the final dimensions of a ceramic brick.

3.8. Leaching test

The results of leaching experiment (Table 7) indicated that hazardous elements such as As, and Pb in ms waste can be stabilized completely within a sintered ceramic body. The concentrations of heavy metals in the leachates of ceramic bricks and sandwich type tiles were found to be extremely low. Furthermore, small increments that occurred in the concentrations of As, Pb, Mn and Zn were attributed to the cement paste containing 10 wt% ms waste.

4. Conclusions

The study showed that ms waste can be utilized as an admixture in the production of ceramic bricks. Mill scale up to 20 wt% amplifies the properties of ceramic bricks in general due to the fluxing action of the waste and to the partial formation of magnesioferrite in the sintered ceramic body fired above 900 °C. Furthermore, the ceramic bricks that were prepared by adding 15–20 wt% ms waste with 0.5 mm of particle size to the clayey material presented average SE up to 4 dB. Ceramic sandwich type tiles of same dimensions containing almost the same amount of ms waste presented average SE up to 8 dB in the same X-band frequency range. For electromagnetic absorption the same trend was followed. The ceramic bricks presented electromagnetic absorption up to 50% while the ceramic sandwich type tiles of same dimensions presented electromagnetic absorption up to 80% with only a small reduction in the stabilization of absorbing electromagnetic radiation performance. Reflection measurements were presented to be almost independent from the increment of addition in ms waste, phenomenon that consolidates the role of ceramic bricks and sandwich type tiles containing ms waste as absorbing building materials. The prepared ceramic sandwich type tiles showed water absorption, firing shrinkage, flexural and compressive strength within accepted limits. Finally, leaching test performed, showed stabilization of all studied toxic elements within the sintered ceramic structure of both ceramic bricks and tiles.

References

[1] J.A. Elder, D.F. Cahill, Biological Effects of Radiofrequency Radiation, Health Effects Research Laboratory, United States Environmental Protection Agency, Research Triangle Park, North Carolina, 1984.
[2] J.D. Hardy, Regulation of body temperature in man—an overview, in: J.A.J. Stolwijk (Ed.), Energy Conservation Strategies in Buildings, University Printing Service CT, New Haven, 1978.
[3] F. Barnes, B. Greenebaum, Biological and Medical Aspects of Electromagnetic Fields, third ed., Taylor & Francis, New York, 2006.
[4] J. Cao, D.D.L. Chung, Use of fly ash as an admixture for electromagnetic interference shielding, Cement Concrete Res. 34 (2004) 1889–1892.
[5] D.D.L. Chung, Materials for electromagnetic interference shielding, J. Mater. Eng. Perform. 9 (2000) 350–354.
[6] M. Oda, Radio wave absorptive building materials for depressing multipath indoors, in: 1999 International Symposium on Electromagnetic Compatibility, 1999, 492–495.
[7] M. Lou, T. Kan, EM wave absorption construction materials containing magnetic media, J. Magn. Mater. Dev. 33 (2002) 13–15.
[8] J. Cao, D.D.L. Chung, Colloidal graphite as an admixture in cement and as a coating on cement for electromagnetic interference shielding, Cement Concrete Res. 33 (2003) 1737–1740.
[9] D.D.L. Chung, Cement reinforced with short carbon fibers: a multifunctional material, Compos. Part B: Eng. 31 (2000) 511–526.
[10] H. Oka, K. Narita, H. Osada, K. Seki, Experimental results on indoor electromagnetic wave absorber using magnetic wood, J. Appl. Phys. 91 (2002) 7008–7010.
[11] G. Bantsis, C. Sikalidis, M. Betsiou, T. Yioultsis, A. Bourliva, Ceramic building materials for electromagnetic interference shielding using metallurgical slags, Adv. Appl. Ceram. 110 (2011) 233–237.
[12] http://www.sidenor.gr, SIDENOR GROUP, 2009.
[13] Routine testing of Ceramic Materials, English China Clays International Company, Corporate Special Publication, Rodway Smith Ltd, Bournemouth, UK, 1977.
[14] Standard test methods for sampling and testing brick and structural clay tile, ASTM C 67-03a, American Society for Testing and Materials, Philadelphia (PA), 2003.

[15] Specification for masonry units. Clay masonry units, BS EN 771-1: Annex C: 2003, Determination of Water absorption, British Standards Institution, London, UK, 2003.
[16] Methods of test for masonry units. Determination of compressive strength, BS EN 772-1:2000, British Standards Institution, London, UK, 2000.
[17] K. Lakshmi, J. Honey, K.T. Mathew, R. Joseph, K.E. George, Microwave absorption, reflection and EMI shielding of PU–PANI composite, Acta Mater. 57 (2009) 371–375.
[18] Characterisation of waste. Leaching. Compliance test for leaching of granular waste materials and sludges. Part 2: One stage batch test at a liquid to solid ratio of 10 l/kg for materials with particle size below 4 mm (without or with size reduction), BS EN 12457-2:2002. British Standards Institution, London, UK, 2002.
[19] S. Al-Otaibi, Recycling steel mill scale as fine aggregate in cement mortars, Eur. J. Sci. R. 24 (2008) 332–338.
[20] C. Favoni, D. Minichelli, F. Tubaro, S. Bruckner, A. Bachiorrini, S. Maschio, Ceramic processing of municipal sewage sludge (MSS) and steelworks slags (SS), Ceram. Int. 31 (2005) 697–702.
[21] S.P.E. Forsmo, Oxidation of magnetite concentrate powders during storage and drying, Int. J. Miner. Process. 75 (2005) 135–144.
[22] S.M. Antao, I. Hassan, J.B. Parise, Cation ordering in magnesioferrite, $MgFe_2O_4$, to 982 °C using in situ synchrotron X-ray powder diffraction, Am. Mineral. 90 (2005) 219–228.
[23] L. Olmedol, G. Chateau, C. Deleuzec, J.L. Forveille, Microwave characterization and modelization of magnetic granular materials, J. Appl. Phys. 73 (1993) 6992–6994.
[24] G. Viau, F. Ravel, P. Achier, Preparation and microwave characterization of spherical and monodisperse Co20Ni80 particles, J. Appl. Phys. 76 (1994) 6570–6572.
[25] J.Y. Shin, J.H. Oh, The microwave absorbing phenomenon of ferrite microwave absorbers, IEEE Trans. Magn. 29 (1993) 3437–3439.
[26] R.M. Cornell, U. Schwertmann, Iron Oxides. Structure, Properties, Reactions Occurrences and Uses, second ed., Wiley-VCH Verlag GmbH & Co. KgaA, Weinheim, 2003.
[27] F. Fiorillo, Measurements and Characterization of Magnetic Materials, Elsevier, Amsterdam, 2004.